N-body Simulations with generic non-Gaussian Initial Conditions

Paper I: arXiv:1006.5793 (JCAP 2010)
Paper II: in preparation

Christian Wagner

with Licia Verde and Lotfi Boubekeur

17 December 2010, Allahabad

Outline

- Introduction
- Initial Condition Generation
- Simulations and numerical Tests
- Results
- Conclusions

Non-Gaussianity

- Non-Gaussian PDF of the density contrast (1-point)
- Skewness $<\delta^3> \neq 0$

  => non-zero bispectrum $B(k_1,k_2,k_3)$ (3-point)
- Non-vanishing higher-order statistics (n-point)

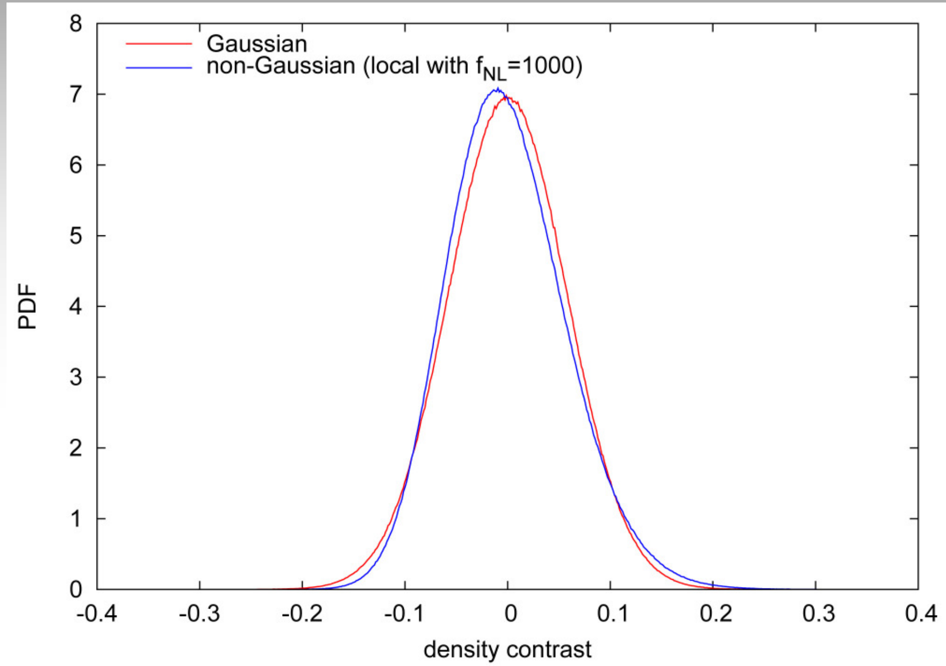

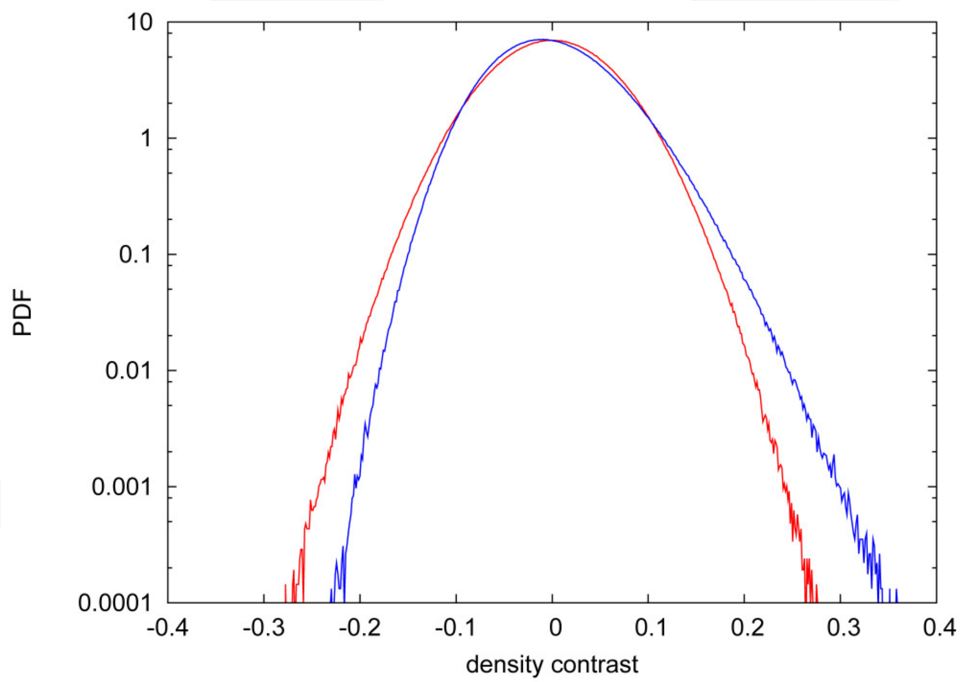

Different shapes

$$\langle \Phi_{k_1}\Phi_{k_2}\Phi_{k_3}\rangle = (2\pi)^3\delta^D(\mathbf{k}_1+\mathbf{k}_2+\mathbf{k}_3)B(k_1,k_2,k_3)$$

Triangle configuration for which the bispectrum peaks

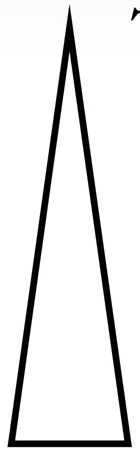

Squeezed / local

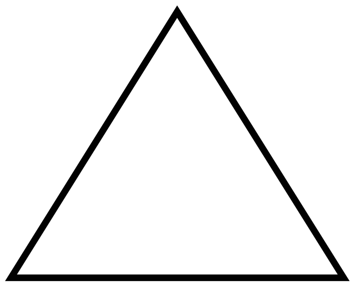

equilateral

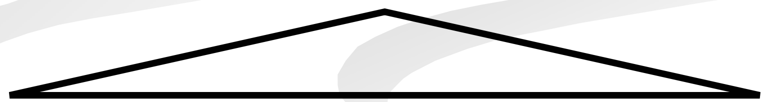

flattened /enfolded

orthogonal (to the equilateral shape)

Probes of non-Gaussianity

- **Cosmic Microwave Background**

$$-10 < f_{NL}^{\text{local}} < 74$$
$$-214 < f_{NL}^{\text{equil}} < 266$$
$$-410 < f_{NL}^{\text{orthog}} < 6$$

(Komatsu et al. 2010)

- **Large-scale structure**:
  - Abundance of very massive objects (or voids)

    Local: $f_{NL} = 449 \pm 286$ (Cayon et al. 2010, see also Hoyle et al. 2010 and Enqvist et al. 2010)

  - Scale-dependent halo bias on large scales

    Local: $-27 < f_{NL} < 70$ (Slosar et al. 2008, see also Xia et al. 2010)

  - Halo bispectrum

    e.g. Nishimichi et al 2009 (simulations) and Baldauf et al. 2010 (PT)

Non-Gaussian halo bias

- Scale-dependent halo bias on large scales (Dalal et al. 2008)
- Local bias approach:

$$\frac{\Delta b_h}{b_h} = \frac{\Delta_c}{D(z)}\beta(k)$$

(Verde and Matarrese 2009)

- Peak Background Split (Slosar et al. 2008, Schmidt et al. 2010)

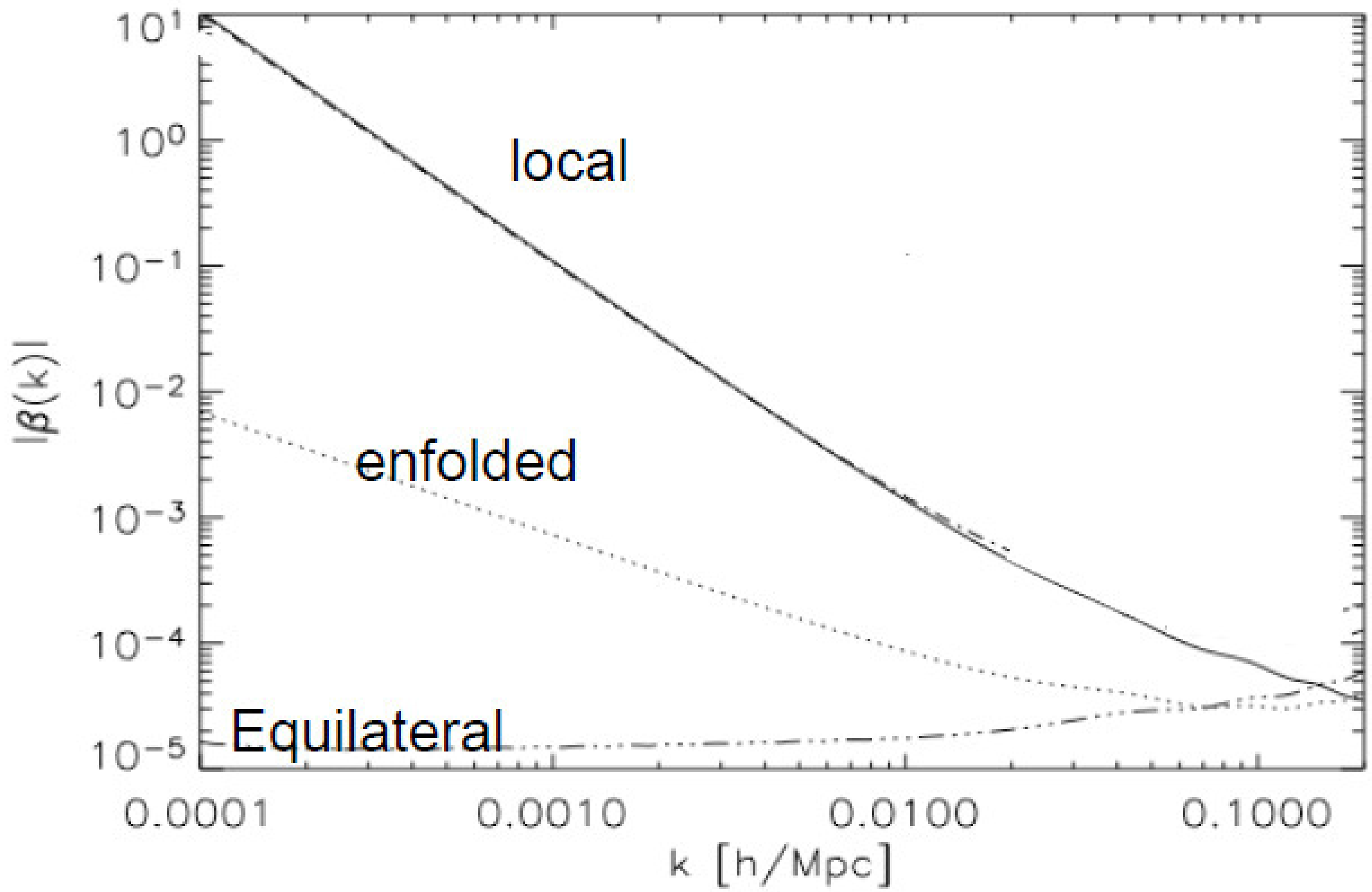

Non-Gaussian halo mass function

- Press-Schechter for non-Gaussian fields
- Two different approximations:
  - MVJ (Matarrese, Verde, Jimenez 2000)
  - LoVerde et al. 2008
- Skewness is the relevant parameter
- For other analytic approaches see Aseem's talk (D'Amico et al. 2010, Ma et al. 2007, De Simone et al. 2007)

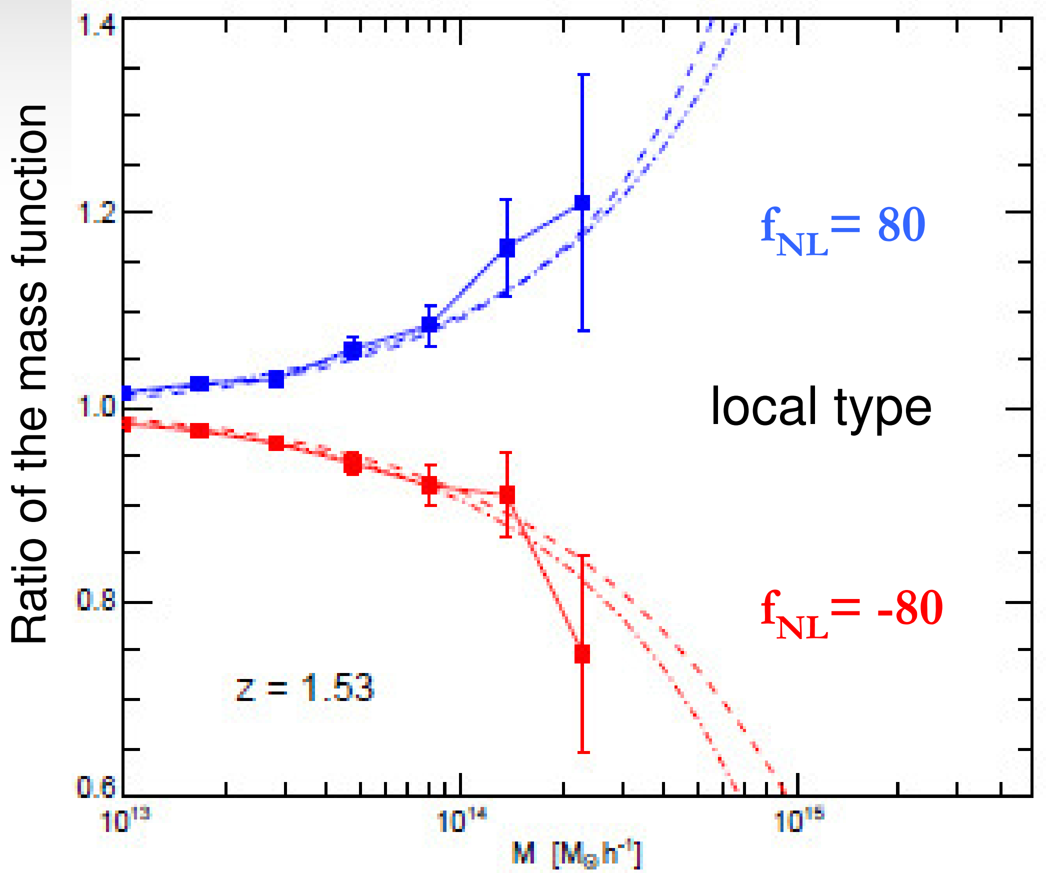

Grossi et al. 2009

N-body Simulations

- Analytic predictions have been tested with N-body simulations by many groups
- Papers:
  - Dalal et al. 2008
  - Grossi et al. 2007 and 2010
  - Desjacques et al. 2009
  - Pillepich et al. 2010
  - …

- But up to now **only the local type** was simulated!

Outline

- Introduction
- Initial Condition Generation
- Simulations and numerical Tests
- Results
- Conclusions

Initial Conditions

- Split the Potential into a Gaussian and a (small) non-Gaussian part

$$\Phi_{\mathbf{k}} = \Phi_{\mathbf{k}}^{G} + \Phi_{\mathbf{k}}^{NG}$$

- Generate a Gaussian Random field

  $\Phi^{G}_{\boldsymbol{k}} \sim N\{0, (P(k)/2)^{1/2}\} + i\, N\{0, (P(k)/2)^{1/2}\}$

  $P(k)=A\, k^{n-4}$ where n is the spectral index

- Poisson equation and CMB physics

$$\delta_{\mathbf{k}} = \frac{2}{3}\frac{k^2 T(k) D(z)}{\Omega_m H_0^2}\Phi_{\mathbf{k}}$$

- Using Zel'dovich Approximation or 2LPT to generate particle distribution

How to get ϕ^{NG}

- Ansatz for Φ^{NG} for a given bispectrum

$$\Phi^{NG}_{\mathbf{k}} = \frac{1}{6(2\pi)^3}\int d^3k_2 d^3k_3 B(k,k_2,k_3)\delta^D(\mathbf{k}+\mathbf{k}_2+\mathbf{k}_3)\frac{\Phi^{*G}_{\mathbf{k_2}}\Phi^{*G}_{\mathbf{k_3}}}{P(k_2)P(k_3)}$$
$$= \frac{1}{6(2\pi)^3}\int d^3k_2 B(k,k_2,|\mathbf{k}+\mathbf{k}_2|)\frac{\Phi^{*G}_{\mathbf{k_2}}}{P(k_2)}\frac{\Phi^{G}_{\mathbf{k}+\mathbf{k_2}}}{P(|\mathbf{k}+\mathbf{k}_2|)}$$

- Test: $\langle \Phi^G_{k_1}\Phi^G_{k_2}\Phi^{NG}_{k_3}\rangle = \frac{1}{3}(2\pi)^3 B(k_1,k_2,k_3)\delta^D(\mathbf{k}_1+\mathbf{k}_2+\mathbf{k}_3)$ ✓

- Does P(k) change?
- Computationally very expensive: cost ~ $N_g^{\;6}$

If the Bispectrum is factorizable

$$B(k_1, k_2, k_3) \equiv \sum_i b_1^i(k_1) b_2^i(k_2) b_3^i(k_3)$$

$$\Phi_{\mathbf{k}}^{NG} = \frac{1}{6} \sum_i b_1^i(k) \int \frac{d^3 k_2}{(2\pi)^3} G^i(\mathbf{k}_2) Q^i(\mathbf{k} + \mathbf{k}_2)$$

- Compute convolutions with the help of Fast Fourier Transforms => very significant speed up of the IC generation

Bispectrum for different shapes

$$B(k_1, k_2, k_3) = 2 f_{\mathrm{NL}}^{\mathrm{local}} F^{\mathrm{local}}(k_1, k_2, k_3)$$

$$B(k_1, k_2, k_3) = 6 f_{\mathrm{NL}}^{\mathrm{eql}} \left(-F^{\mathrm{local}} - 2F^A + F^B\right)$$

$$B(k_1, k_2, k_3) = 6 f_{\mathrm{NL}}^{\mathrm{enfl}} \left(F^{\mathrm{local}} + 3F^A - F^B\right)$$

$$B(k_1, k_2, k_3) = 6 f_{\mathrm{NL}}^{\mathrm{orth}} \left(-3F^{\mathrm{local}} - 8F^A + 3F^B\right)$$

$$F^{\mathrm{local}}(k_1, k_2, k_3) = P(k_1)P(k_2) + P(k_2)P(k_3) + P(k_1)P(k_3)$$

$$F^A(k_1, k_2, k_3) = [P(k_1)P(k_2)P(k_3)]^{2/3}$$

$$F^B(k_1, k_2, k_3) = \{[P(k_1)]^{1/3}[P(k_2)]^{2/3}P(k_3) + 5\mathrm{cyc.}\}$$

Local case

- local a) $$\Phi(\mathbf{x}) = \Phi^G(\mathbf{x}) + f_{\rm NL}(\Phi^G(\mathbf{x})^2 - \langle\Phi^G(\mathbf{x})^2\rangle)$$

(in real space)

- local b) $$B(k_1,k_2,k_3) = 2 f_{\rm NL}^{\rm local} F^{\rm local}(k_1,k_2,k_3)$$

- local c) $$B(k_1,k_2,k_3) \longrightarrow 6 f_{\rm NL} P(k_2) P(k_3)$$

$$\Phi_{\mathbf{k}} = \Phi_{\mathbf{k}}^G + f_{\rm NL}\frac{1}{(2\pi)^3}\int d^3k' \Phi_{\mathbf{k}'}^{*G}\Phi_{\mathbf{k}+\mathbf{k}'}^G$$

Variance and skewness

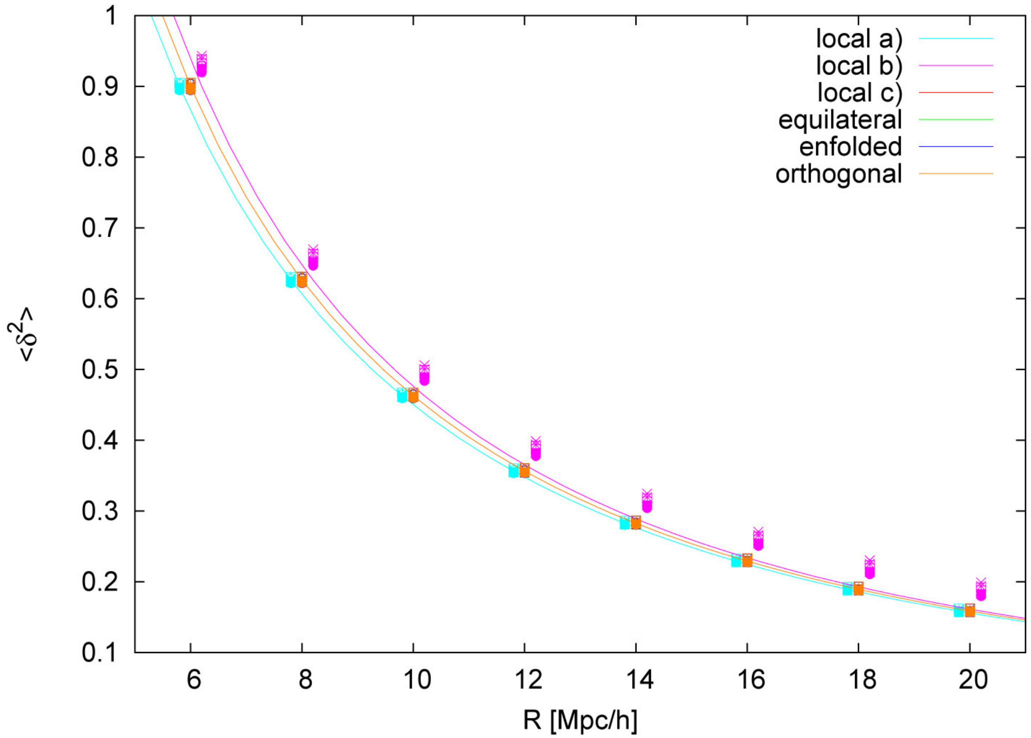

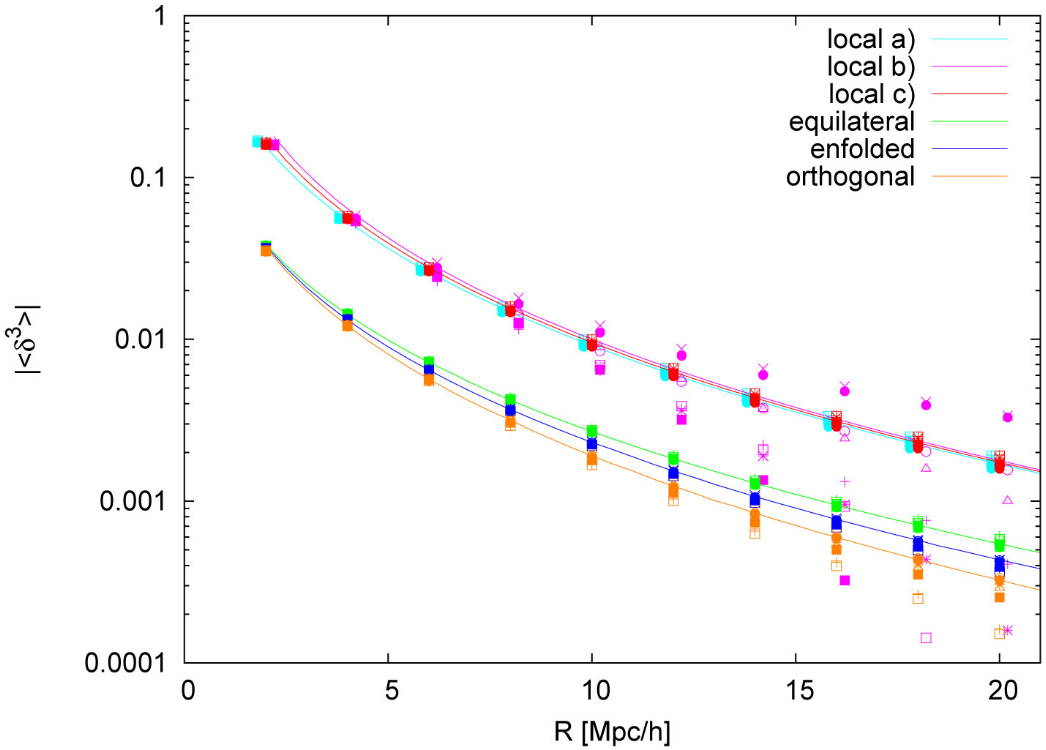

R is the radius of the top-hat filter used to smooth the density field

Initial Power Spectrum

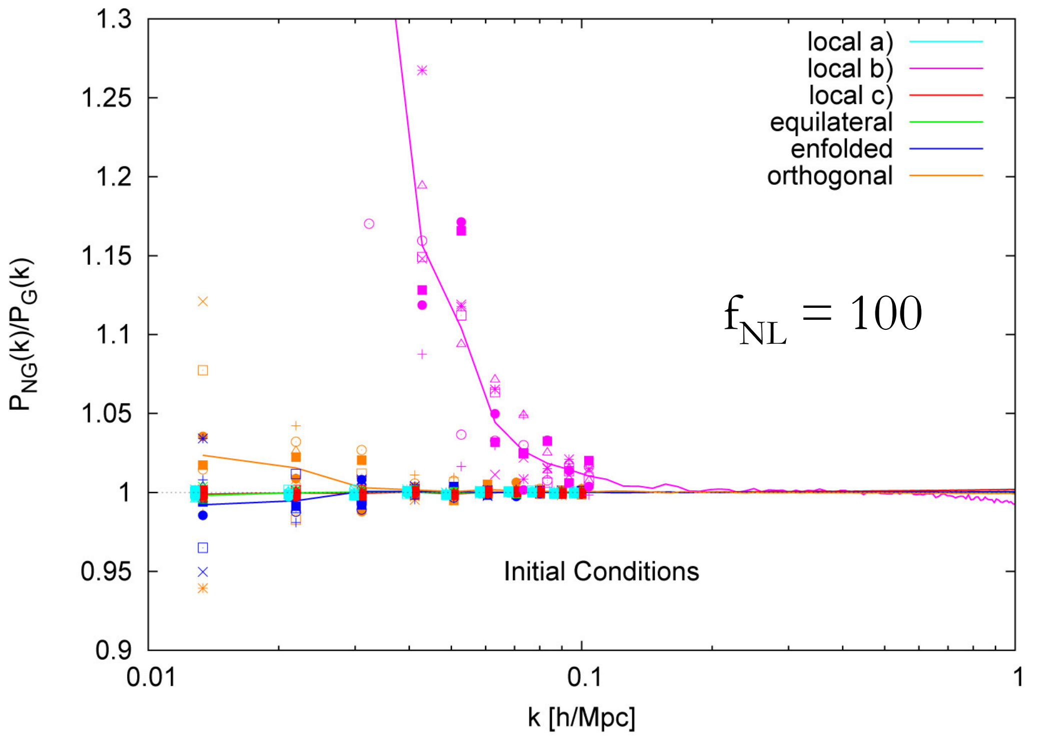

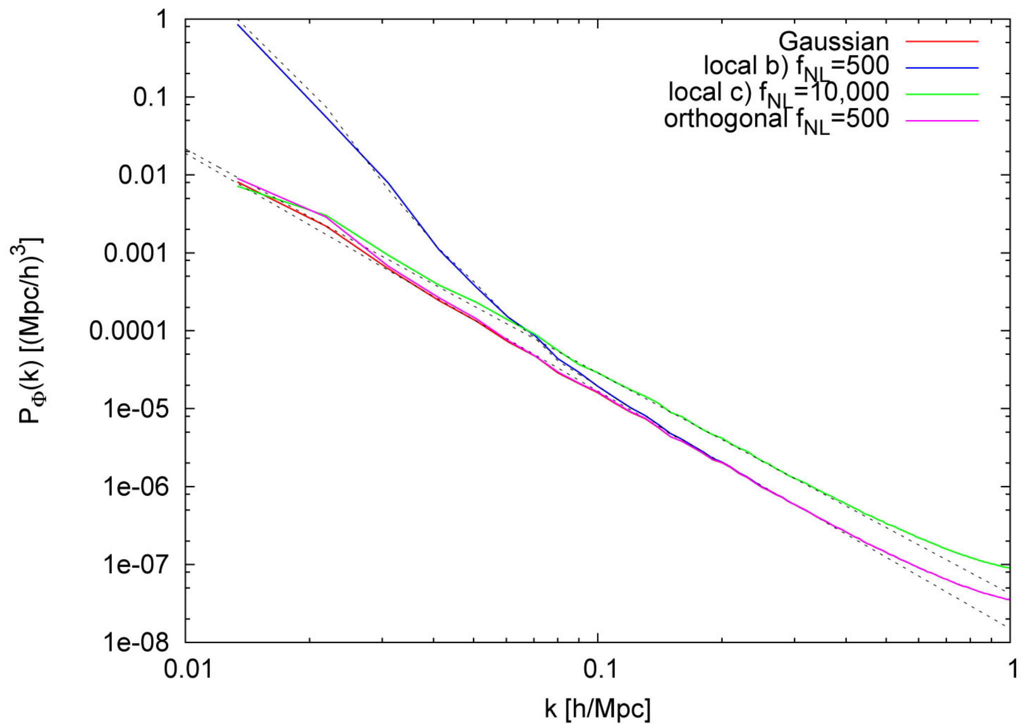

- Second-order terms for "local b)"

$$\langle \Phi^{NG}_{\mathbf{k}} \Phi^{NG}_{\mathbf{q}} \rangle = \frac{2}{9} f_{\rm NL}^2 \delta^D(\mathbf{k}+\mathbf{q}) \left\{ \int d^3k' P(k') P(|\mathbf{k}+\mathbf{k}'|) \right.$$
$$+ 4P(k) \int d^3k' P(k')$$
$$\left. +2P^2(k) \int d^3k' \left(\frac{P(|\mathbf{k}+\mathbf{k}'|)}{P(k')} + 1 \right) \right\}$$

Outline

- Introduction
- Initial Condition Generation
- Simulations and numerical Tests
- Results
- Conclusions

Simulations

Table 1. Settings of the N-body simulations.

$N_{\rm part}$	$L_{\rm box}$ (Mpc/h)	$m_{\rm part}$ ($M_\odot/h$)	$l_{\rm soft}$ (kpc/h)	$z_{\rm initial}$	$f_{\rm NL}$	shape	# sims
256^3	600	10^{12}	70	49	-500 to 500^a	local c)	8
256^3	600	10^{12}	70	49	-500 to 500^a	equilateral	8
256^3	600	10^{12}	70	49	-500 to 500^a	enfolded	8
256^3	600	10^{12}	70	49	-500 to 500^a	orthogonal	8
512^3	600	$\sim 10^{11}$	35	49	0 and 100	local a)	1
512^3	1200	10^{12}	70	49	0 and 100	local a)	1
256^3	600	10^{12}	70	99	0 and 100	local a)	1
256^3	600	10^{12}	70	49	0 and 100	local a)	1

[a] $f_{\rm NL} = -500, -250, -100, 0, 100, 250, 500$

Non-linear Power Spectrum

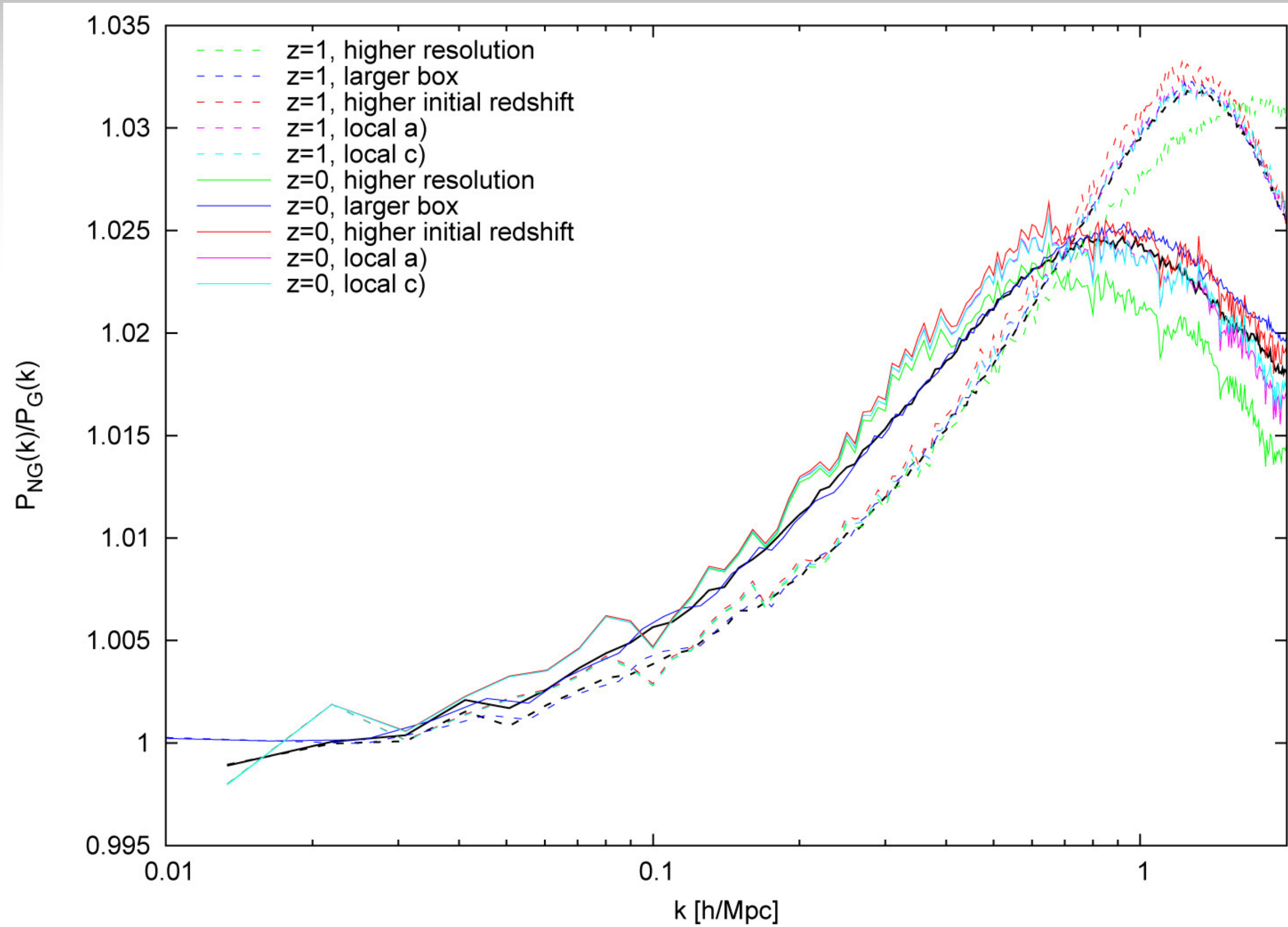

Halo Mass Function

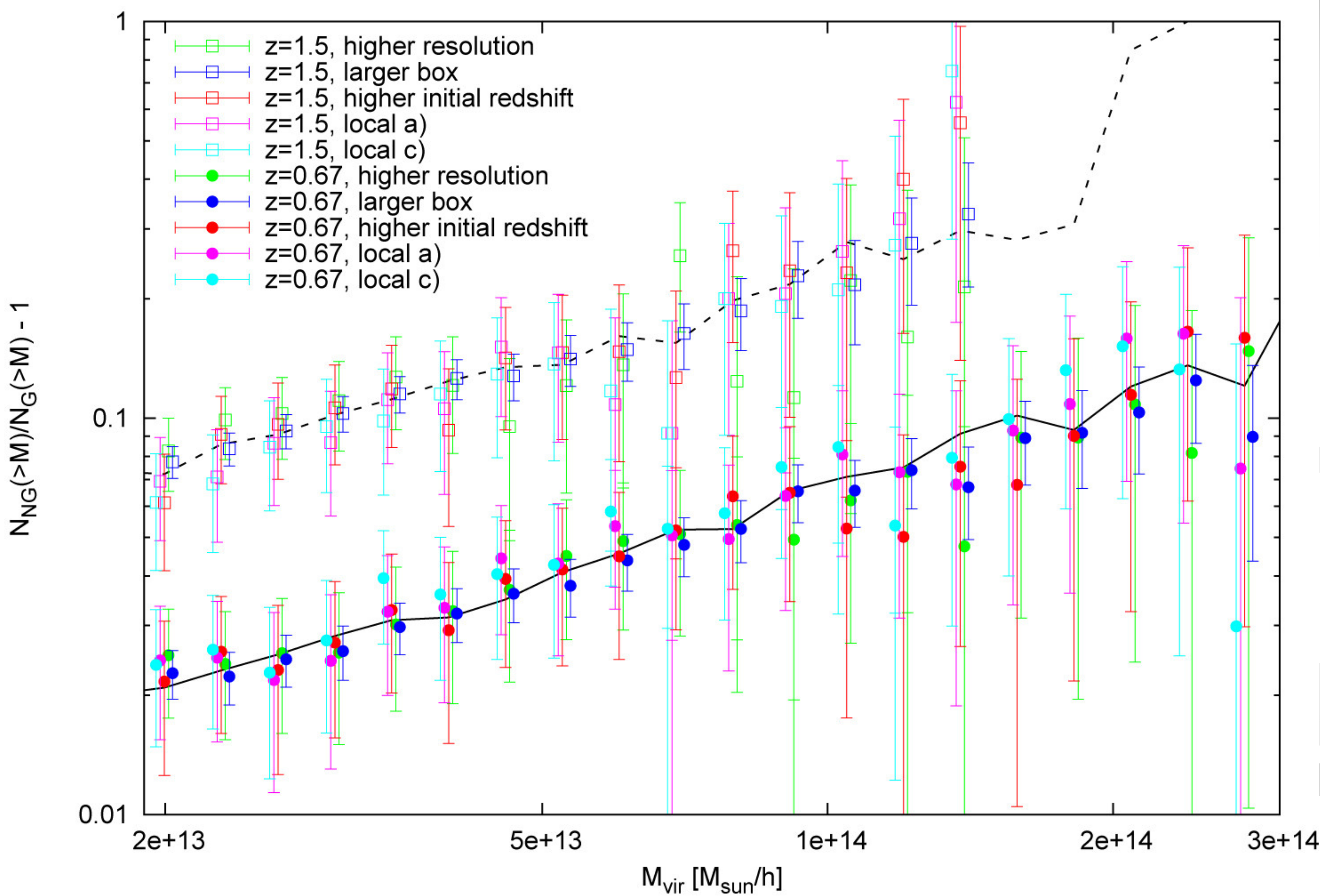

Outline

- Introduction
- Initial Condition Generation
- Simulations and numerical Tests
- Results
- Conclusions

Non-linear Power spectrum

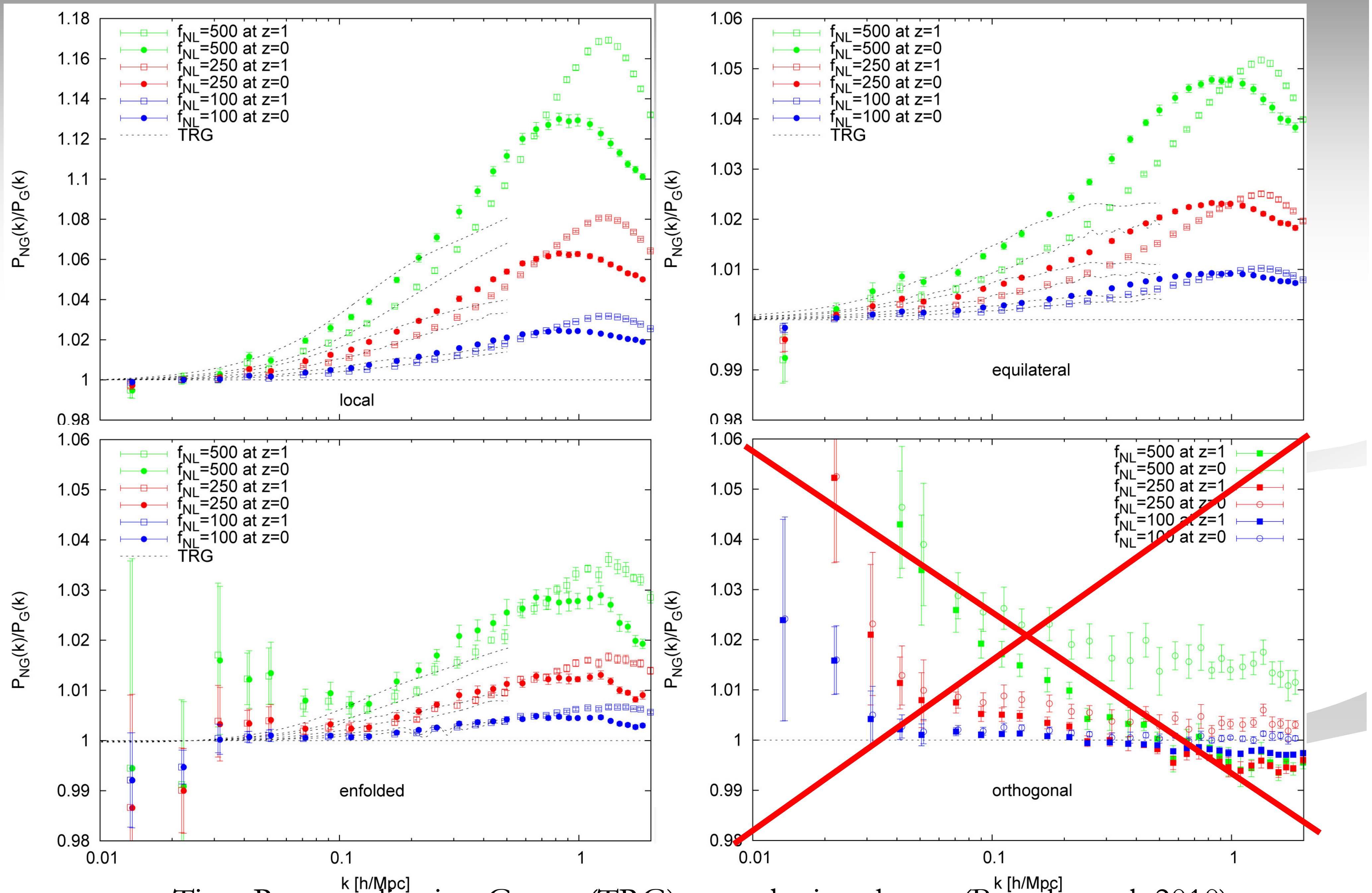

Time Renormalization Group (TRG) perturbation theory (Bartolo et al. 2010)

Halo mass function

- Here, halos are defined as bound objects with an spherical overdensity equal to the virial density (instead of Friends-of-Friends halos)

No $\delta_c \longrightarrow \sqrt{q}\delta_c$?

- Theoretical Predictions for the ratio of *cumulative* mass functions

$$R_{NG}(>M) = \frac{\int_M^\infty r_{NG}(\tilde{M}) n_{\text{Tinker}}(\tilde{M}) d\tilde{M}}{\int_M^\infty n_{\text{Tinker}}(\tilde{M}) d\tilde{M}}$$

with $r_{NG}(M)$ the ratio:

MVJ

$$r_{NG}(M,z,f_{NL}) = \exp\left[\delta_{ec}^3 \frac{S_{3,M}}{6\sigma_M^2}\right] \times$$
$$\left|\frac{1}{6}\frac{\delta_{ec}^2}{\sqrt{1-\delta_{ec}S_{3,M}/3}}\frac{dS_{3,M}}{d\ln\sigma_M} + \frac{\delta_{ec}\sqrt{1-\delta_{ec}S_{3,M}/3}}{\delta_{ec}}\right|$$

LV

$$r_{NG}(M,z,f_{NL}) = 1 + \frac{1}{6}\frac{\sigma_M^2}{\delta_{ec}} \times$$
$$\left[S_{3,M}\left(\frac{\delta_{ec}^4}{\sigma_M^4} - 2\frac{\delta_{ec}^2}{\sigma_M^2} - 1\right) + \frac{dS_{3,M}}{d\ln\sigma_M}\left(\frac{\delta_{ec}^2}{\sigma_M^2} - 1\right)\right]$$

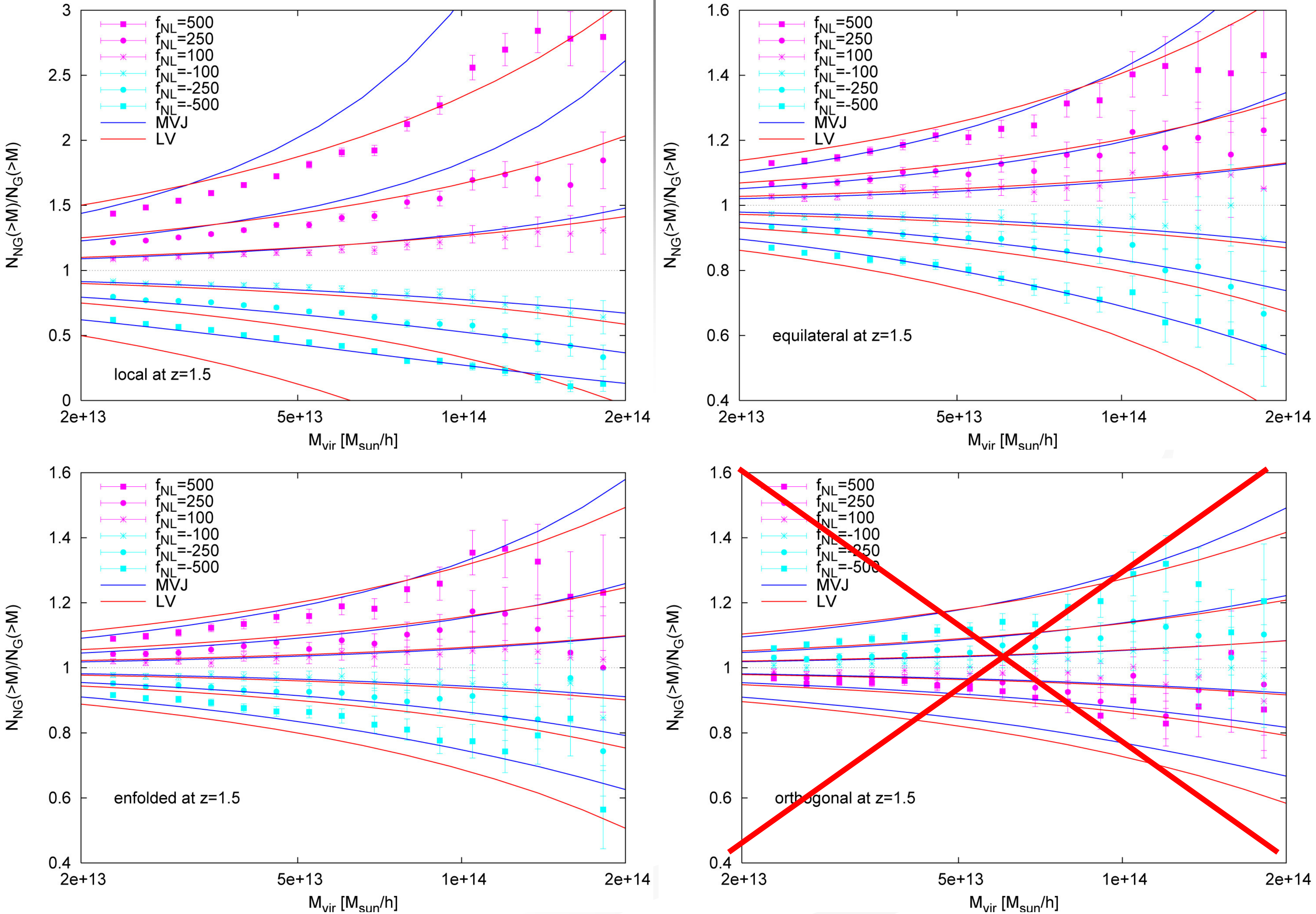

fNL=500
fNL=250
fNL=100
fNL=-100
fNL=-250
fNL=-500
MVJ
LV
local at z=1.5
equilateral at z=1.5
enfolded at z=1.5
orthogonal at z=1.5
NNG(>M)/NG(>M)
Mvir [Msun/h]
2e+13
5e+13
1e+14
2e+14

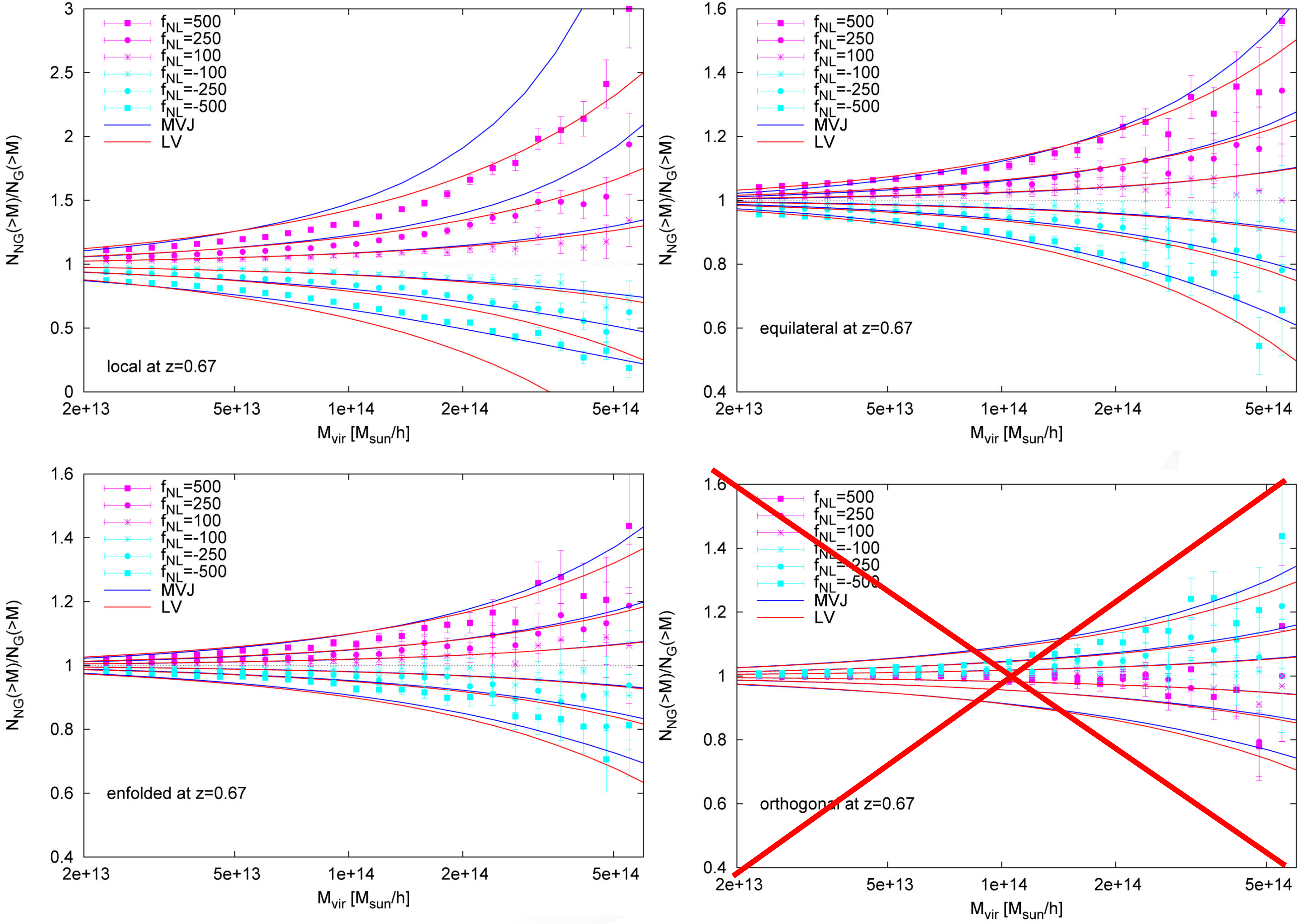

fNL=500
fNL=250
fNL=100
fNL=-100
fNL=-250
fNL=-500
MVJ
LV
NNG(>M)/NG(>M)
Mvir [Msun/h]
local at z=0.67
equilateral at z=0.67
enfolded at z=0.67
orthogonal at z=0.67

NG halo bias

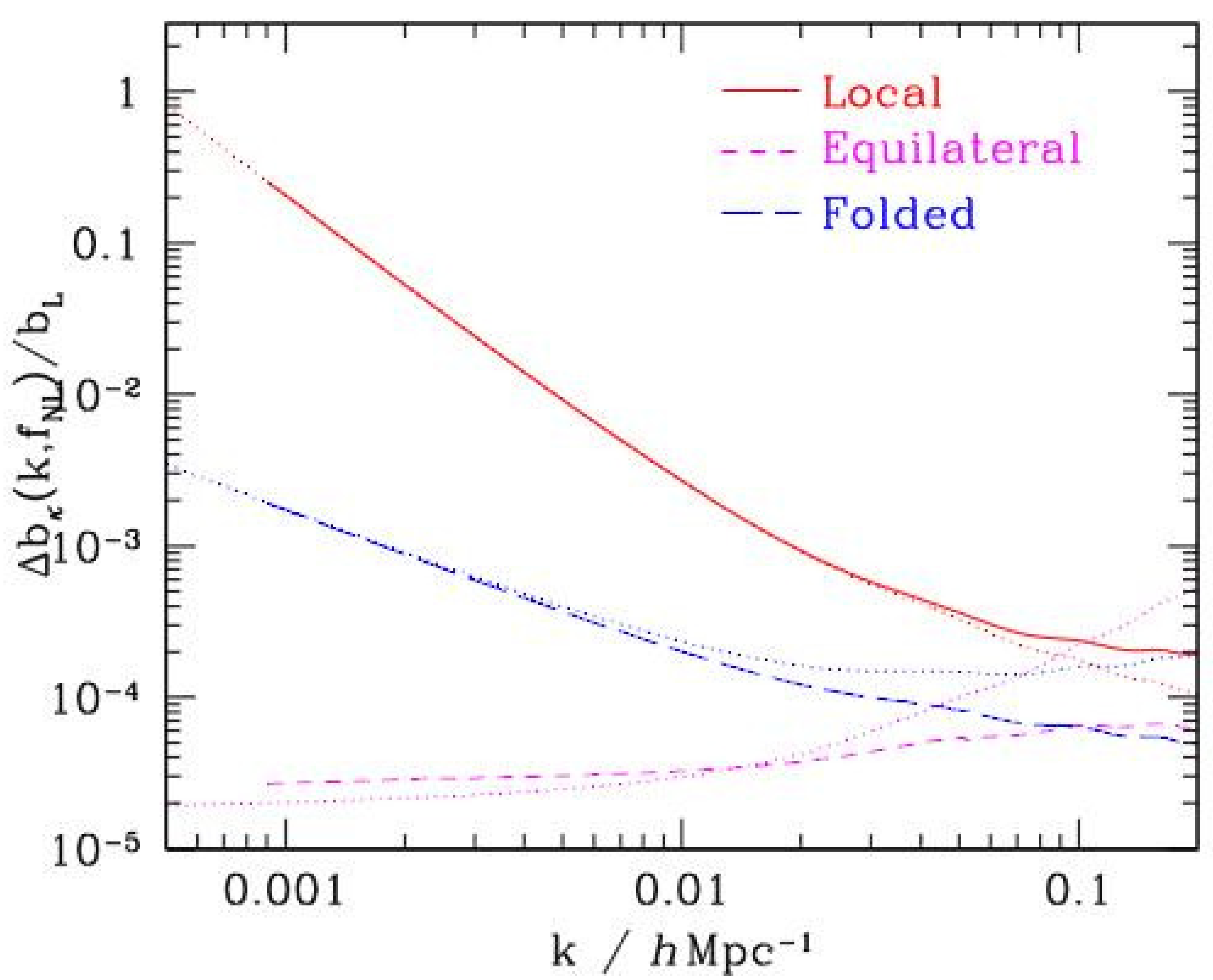

from a review article by Desjacques and Seljak (2010)

- NG halo bias depends on shape
- Effect becomes measurable on large scales
- linear in f_{NL}

NG halo bias

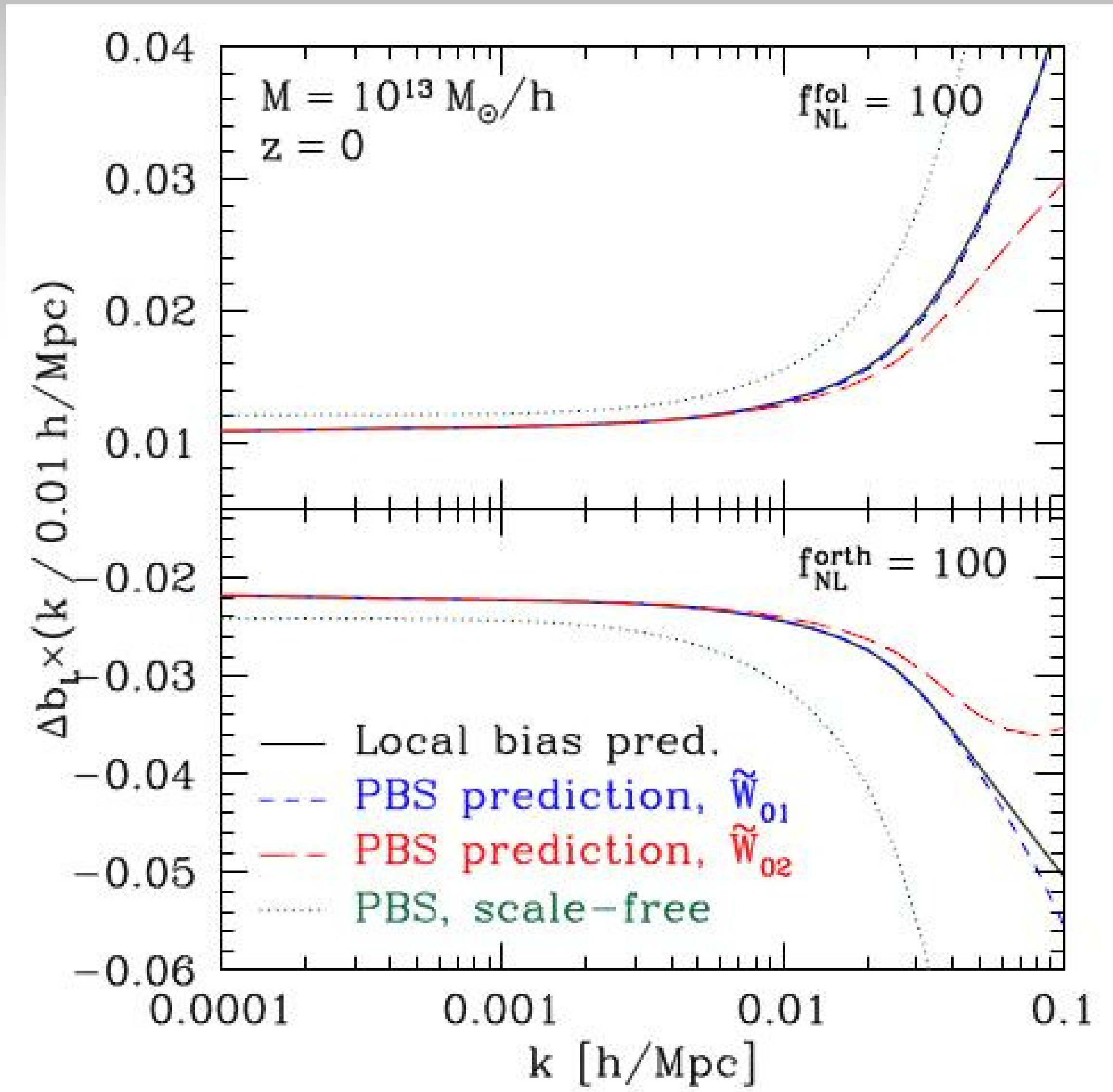

Prediction derived with the **peak backgound split** approach
Schmidt & Kamionkowski (2010)

Templates vs. physical shapes

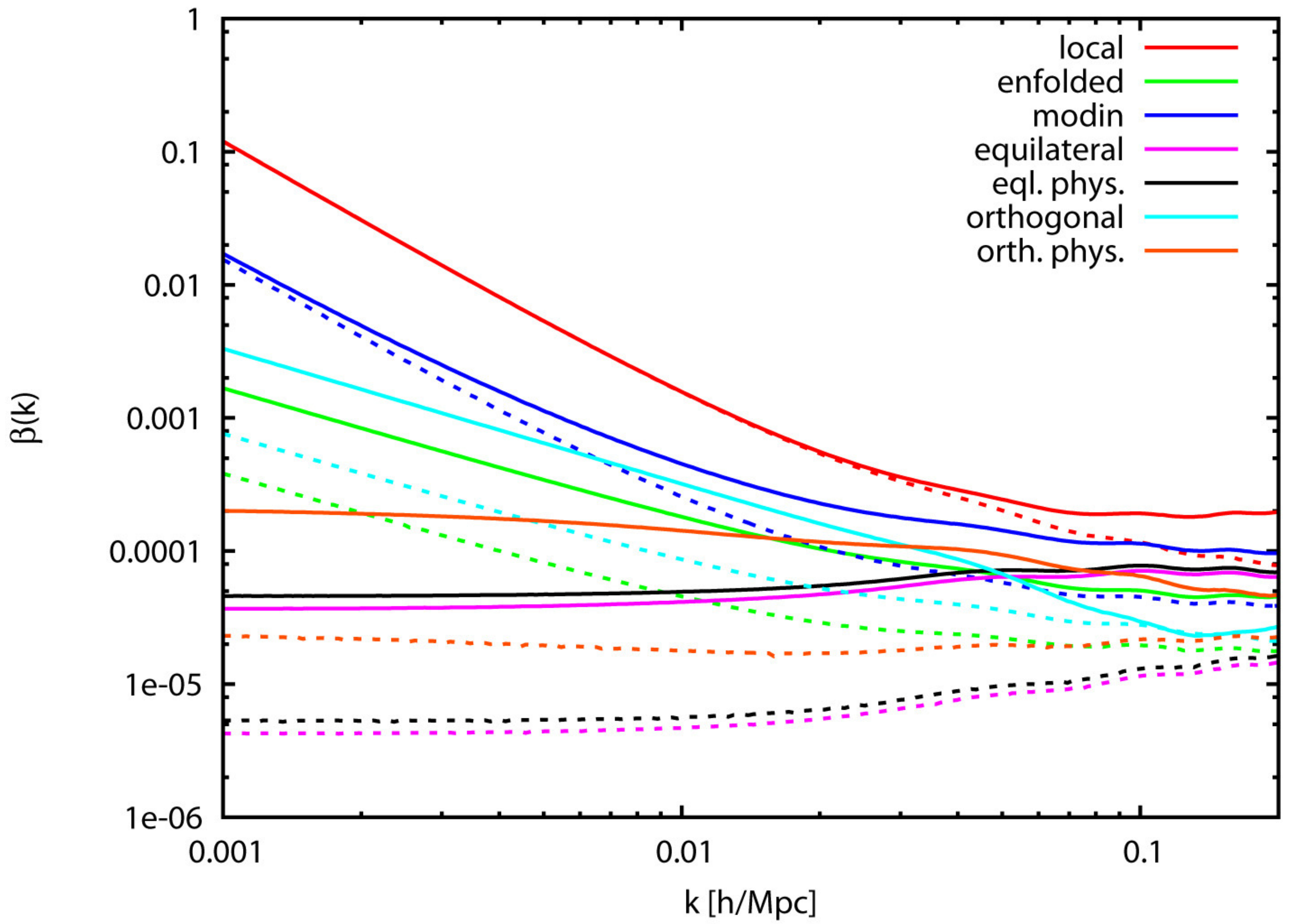

solid lines: R=10 Mpc/h dashed lines: R=1 Mpc/h

- modified initial state / enfolded (Meerburg et al. 2009)
- orthogonal and equilateral (Senatore et al. 2010)
- templates maximize the so-called "cosine", this is relevant for CMB analysis
- for NG bias the correct scaling in the squeezed limit is crucial

Problem

- Second-order contributions of our ansatz

$$\langle \Phi_{\mathbf{k}}^{NG} \Phi_{\mathbf{q}}^{NG} \rangle = \frac{1}{18} \delta^D(\mathbf{k}+\mathbf{q}) \int d^3k' \frac{B^2(k,k',|\mathbf{k}+\mathbf{k}'|)}{P(k')P(|\mathbf{k}+\mathbf{k}'|)}$$

scale a $\mathbf{f_{NL}}^2/\mathbf{k}$ for the enfolded and orthogonal template

- The NG halos bias scales as $\mathbf{f_{NL}}/\mathbf{k}$

=> Effect is swamped by artificial power on large scales

Outline

- Introduction
- Initial Condition Generation
- Simulations and numerical Tests
- Results
- Conclusions

Modified Ansatz

- Generalize the transformation for the local shape:

$$2\left(P(k_1)P(k_2) + P(k_2)P(k_3) + P(k_1)P(k_3)\right) \longrightarrow 6P(k_2)P(k_3)$$

$$\Phi^{NG}_{\mathbf{k_1}} = \frac{1}{2(2\pi)^3}\int d^3k_2 d^3k_3 \frac{B(k_1,k_2,k_3)\delta^D(\mathbf{k}_1+\mathbf{k}_2+\mathbf{k}_3)\Phi^{*G}_{\mathbf{k_2}}\Phi^{*G}_{\mathbf{k_3}}}{P(k_1)P(k_2)+P(k_2)P(k_3)+P(k_1)P(k_3)}$$

(see also Schmidt & Kamionkowski 2010)

- Not factorizable => computational expensive
  - But physical shapes often not factorizable anyway
- Second-order contributions to the Power Spectrum are suppressed on large scales

Using a smaller grid for ϕ_k^{NG}

- ϕ_k^{NG} computation scales as $\sim N_g^6$
- Choose a grid size for ϕ_k^{NG} of 400 (computation takes 2 days on 256 cores)
- Gaussian grid size is 1024
- Box size 1875 Mpc/h
  => "NG resolution" 5 Mpc/h ~ 3×10^{13} M_{sun}/h
- One billion particles per simulation
  => Particle mass ~ 5×10^{11} M_{sun}/h
- Numerical tests confirmed the expected lower mass limit of resolved halos to be **3×10^{13} M_{sun}/h**

Outline

- Introduction
- Initial Condition Generation
- Simulations and numerical Tests
- Results
- Conclusions

NG halo bias

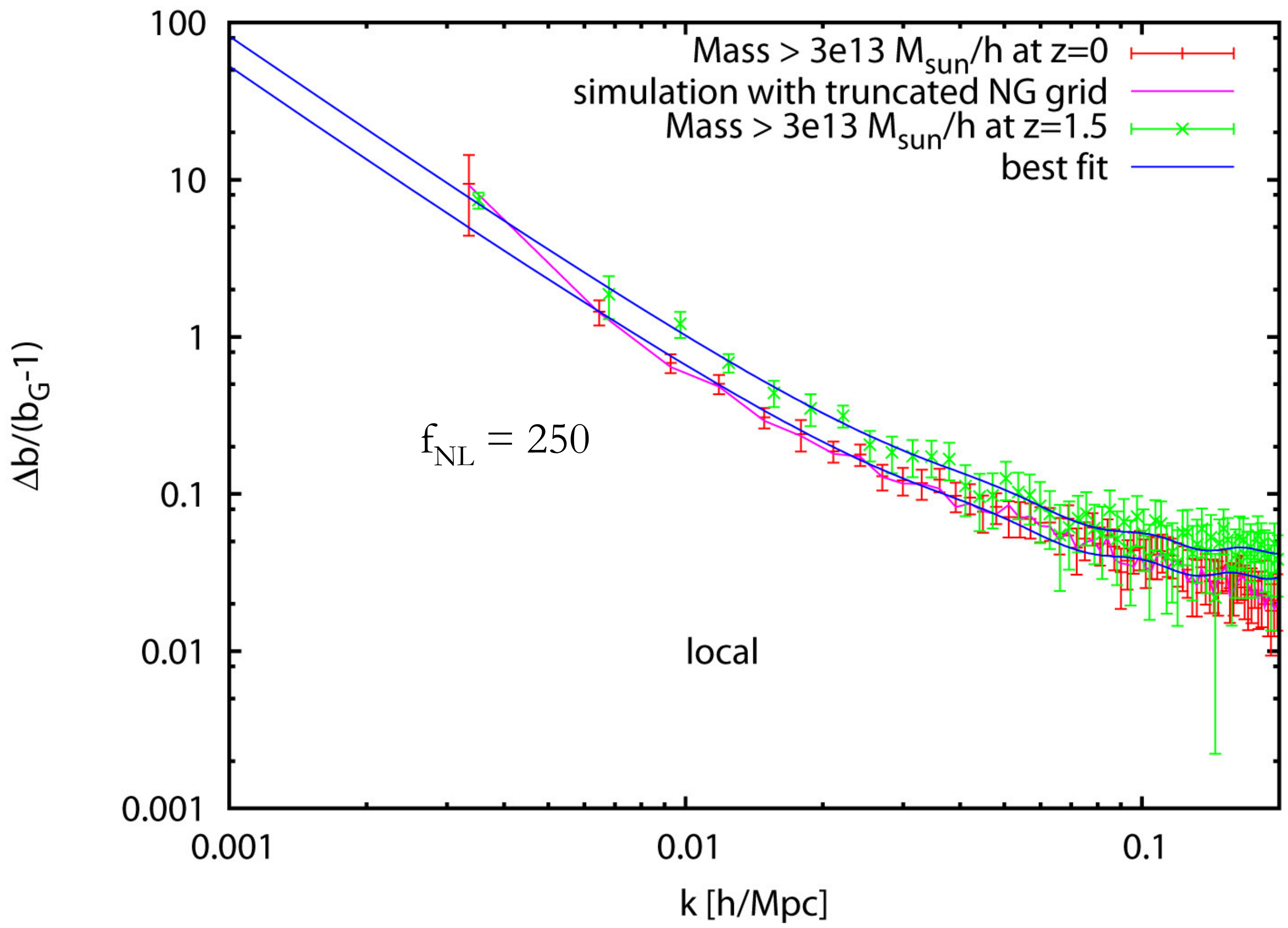
Mass > 3e13 M$_{sun}$/h at z=0
simulation with truncated NG grid
Mass > 3e13 M$_{sun}$/h at z=1.5
best fit
$f_{NL} = 250$
local
$\Delta b/(b_G-1)$
k [h/Mpc]
100
10
1
0.1
0.01
0.001
0.001
0.01
0.1

NG halo bias

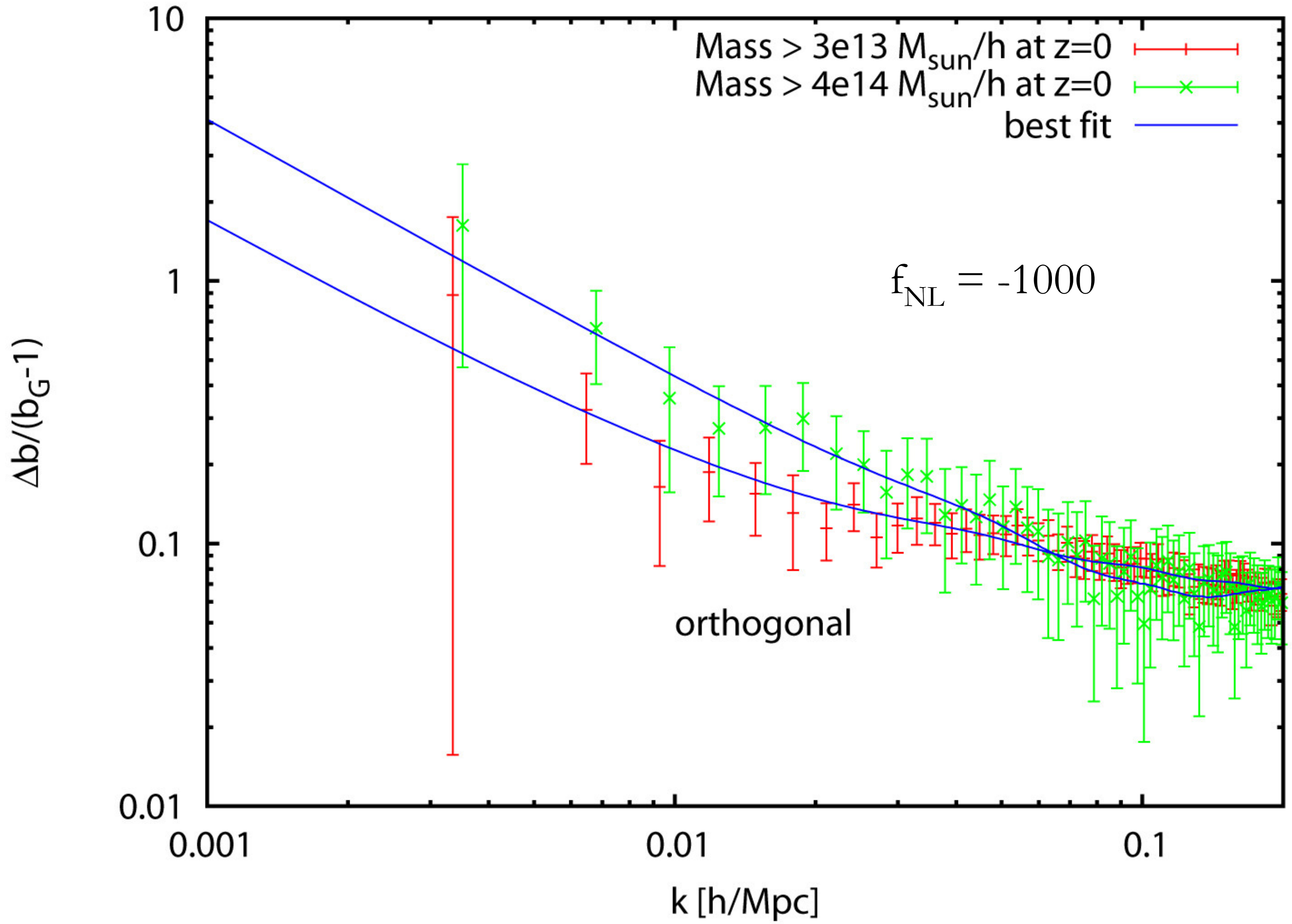

Mass > 3e13 M_sun/h at z=0
Mass > 4e14 M_sun/h at z=0
best fit
f_{NL} = -1000
orthogonal
Δb/(b_G-1)
k [h/Mpc]
10
1
0.1
0.01
0.001
0.01
0.1

NG halo bias

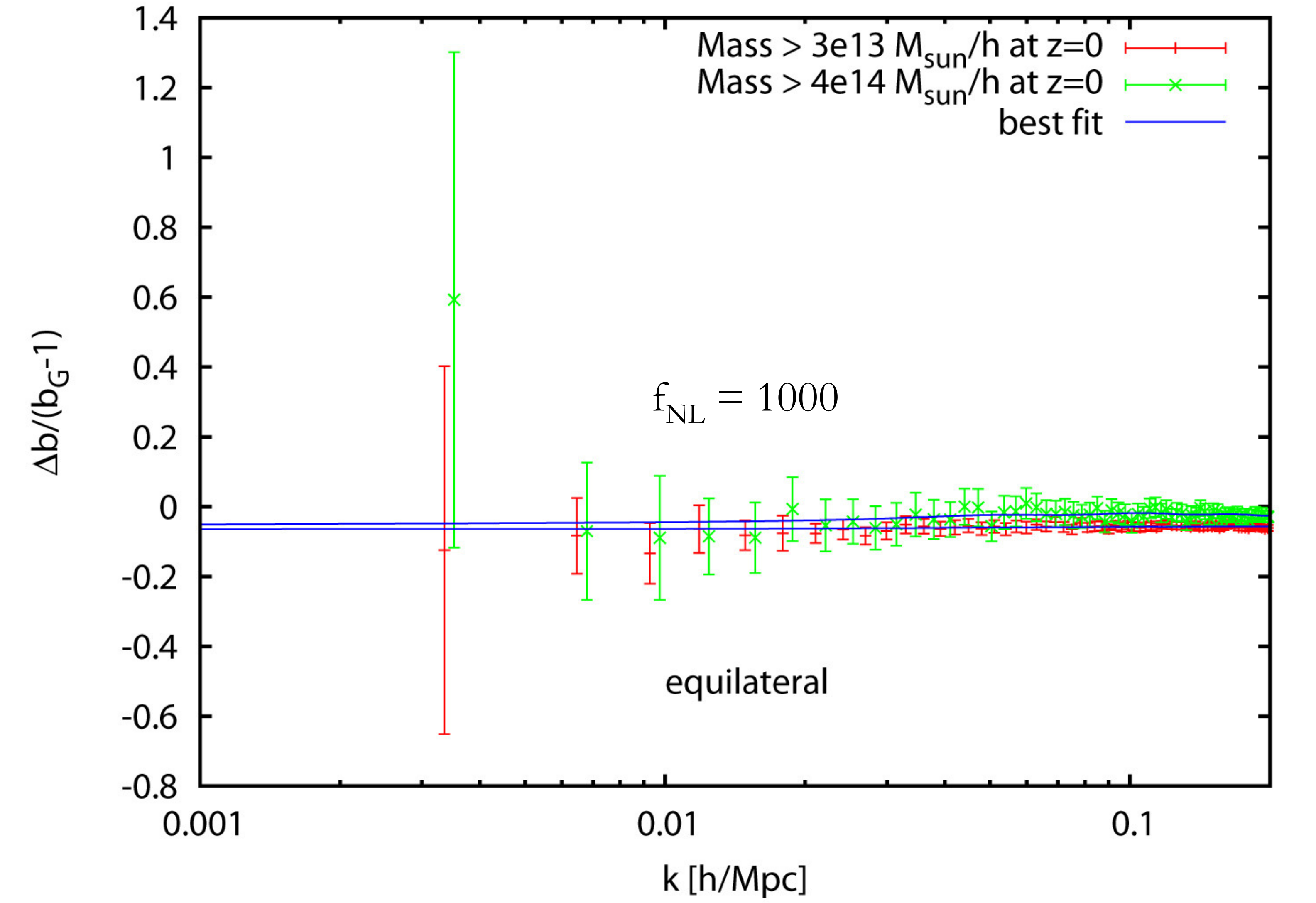

Mass > 3e13 M_sun/h at z=0
Mass > 4e14 M_sun/h at z=0
best fit
Δb/(b_G-1)
f_NL = 1000
equilateral
k [h/Mpc]
1.4
1.2
1
0.8
0.6
0.4
0.2
0
-0.2
-0.4
-0.6
-0.8
0.001
0.01
0.1

NG halo bias

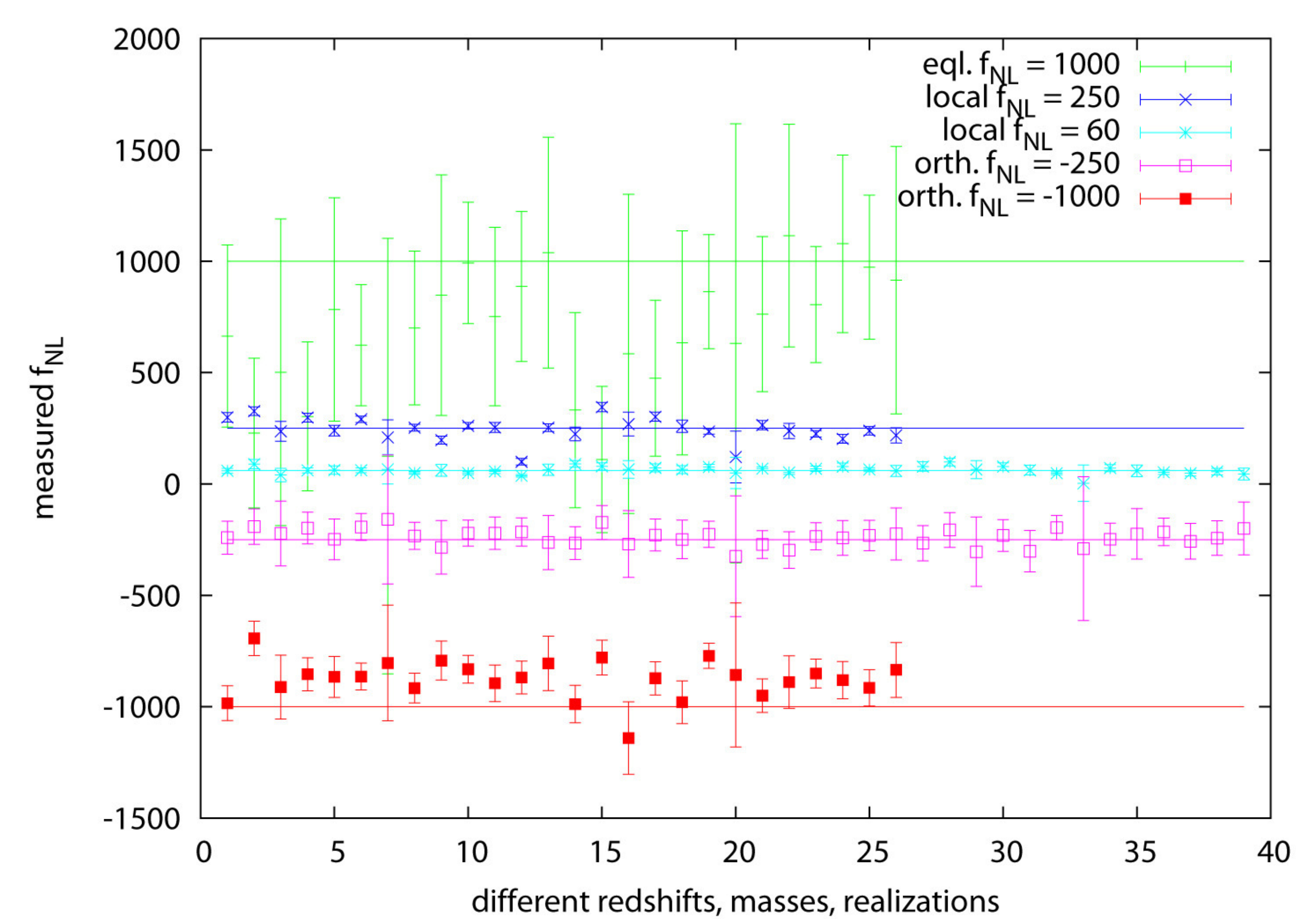

- No significant additional dependence on mass or redshift detected
- Measured fNL values for the orthogonal shape seem to be to low => is the q-correction shape dependent?

Mass function for the local type

z=1.5

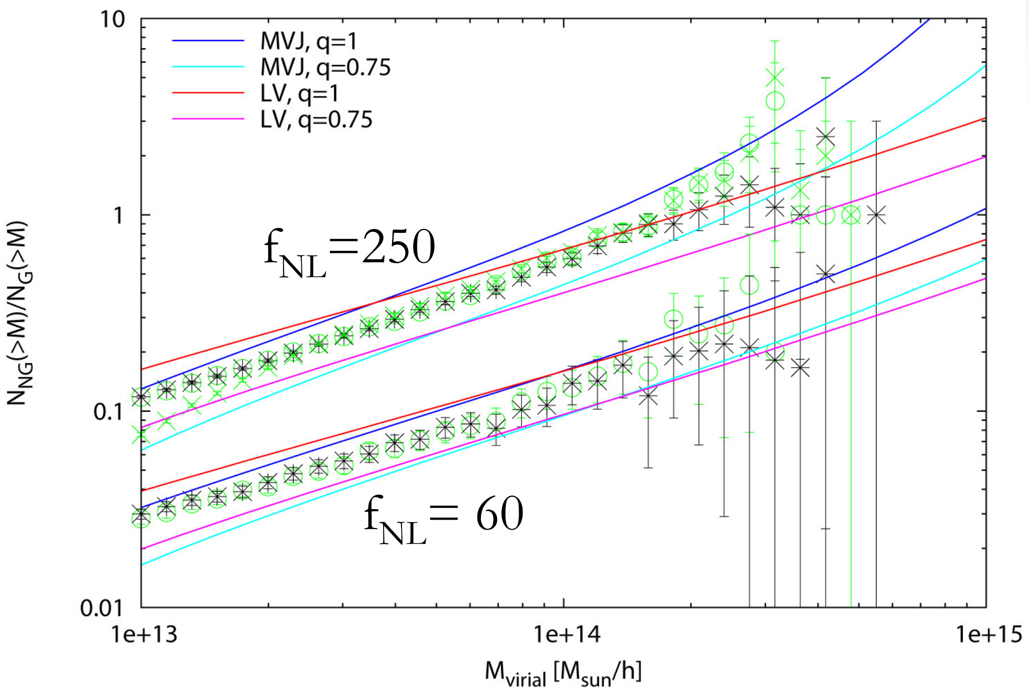

z=0.67

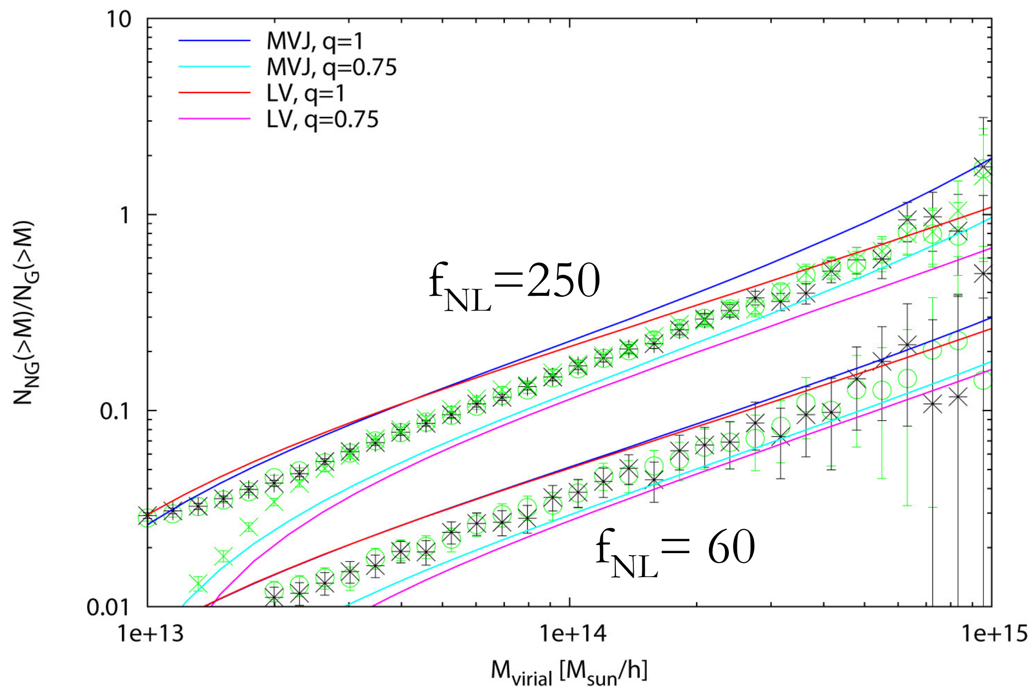

q ~ 0.9 ?

Mass function for the equilateral type

z=1.5

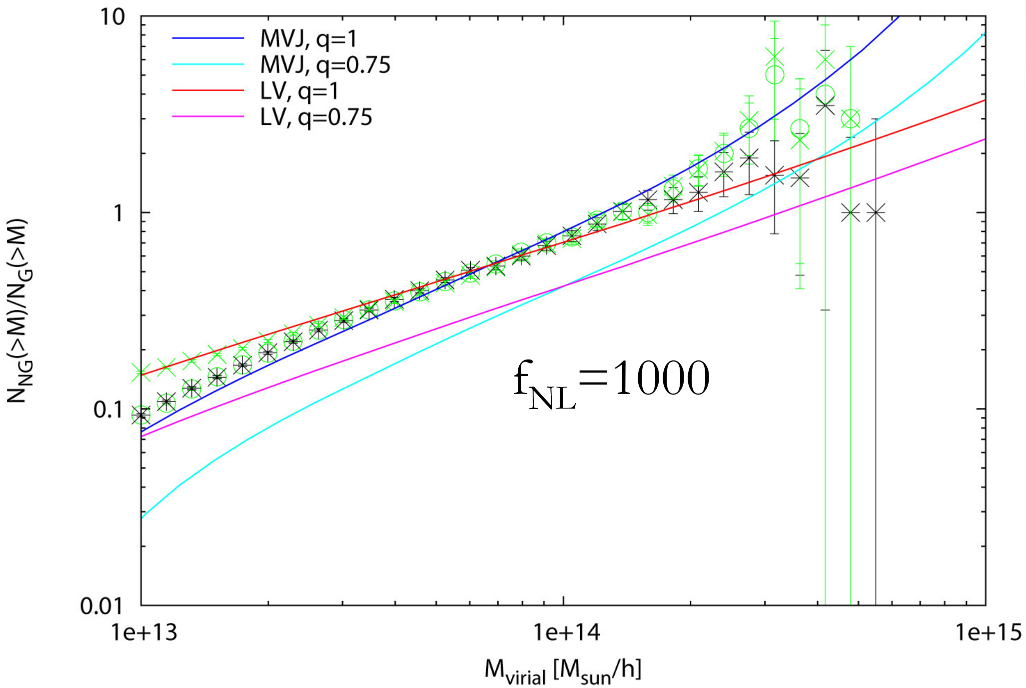

z=0.67

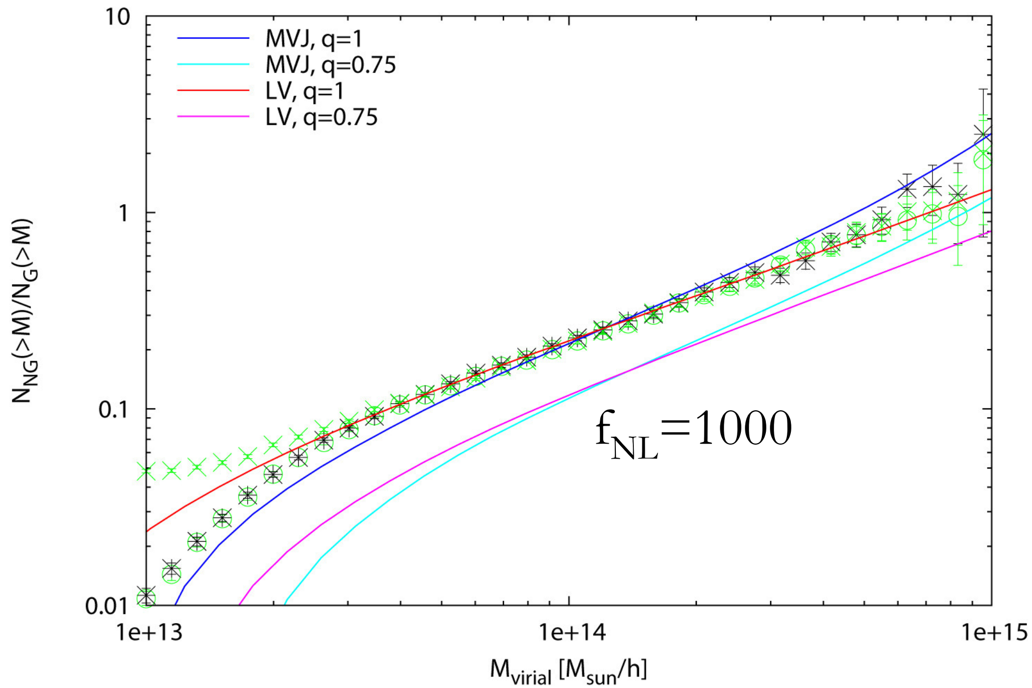

q ~ 1

Mass function for the orthogonal type

z=1.5

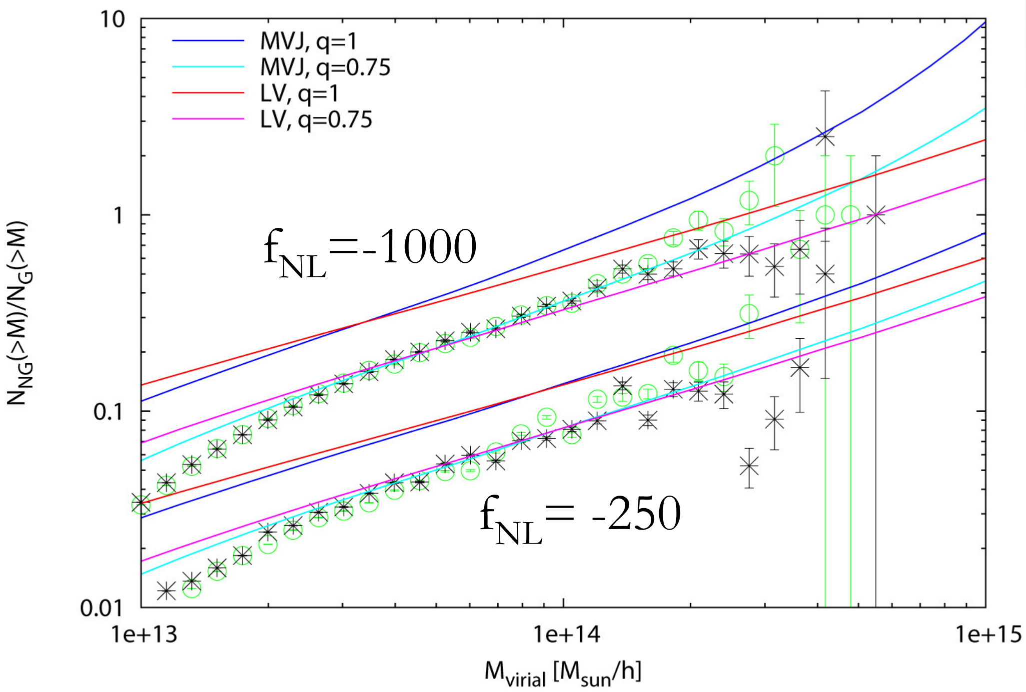

z=0.67

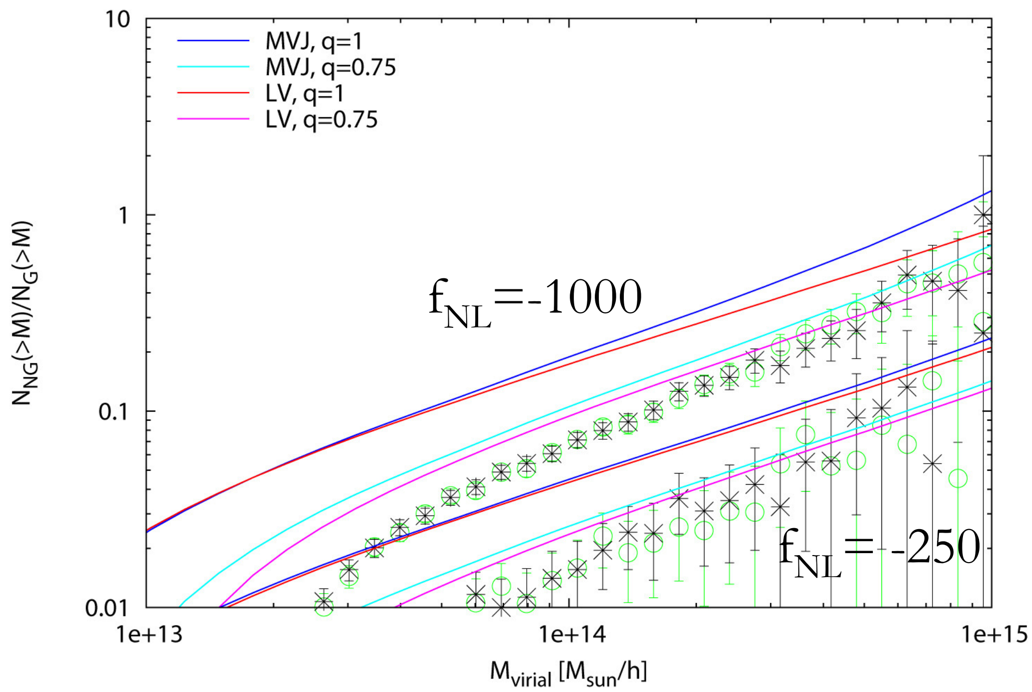

q ~ 0.75 and redshift dependent?

Conclusions

- Non-Gaussian Initial Condition for N-body simulations with generic bispectrum possible, but in most cases computationally expensive
- N-body results for non-local NG are fairly consistent with theoretical predictions
- Mass function predictions need q-calibration

  => Is there a NG shape dependence of the mass function which is not modeled by the skewness?
- Halo bias for non-local shapes needs to be derived from the physical models, not from the CMB templates
- q-correction seems to be shape dependent